

## On Stationarizability for Nonstationary 2-D Random Fields Using Discrete Wavelet Transforms

Bing-Fei Wu and Yu-Lin Su

**Abstract**—The emphasis in this correspondence is on the study of nonstationary two-dimensional (2-D) random fields with wide-sense stationary increments, wide-sense stationary jumps, and 2-D fractional Brownian motion (fBm) fields. The effort made in this work is to develop a realizable method of stationarization provided for nonstationary 2-D random fields. We also present the correlation functions of the discrete wavelet transform relating to 2-D fBm fields that will decay hyperbolically fast.

**Index Terms**—Discrete wavelet transform, nonstationarity, random fields.

### I. INTRODUCTION

The concept of stationarization established herein is based on two motivations. First, lacking of stationarity for a two-dimensional (2-D) random field will cause lacking of time-invariance that is usually found in estimators and detectors. Second, the stationarity is useful in improving the computation efficiency of filters.

Multiresolution signal processing has been used to implement the discrete wavelet transform (DWT) efficiently with almost no redundancy. Through the multiresolution analysis [2, pp. 119–121] [4, pp. 129–166], the DWT performs well in the structure of the subband filter system, called *perfect reconstruction-quadrature mirror filter* (PR-QMF) [12], which is recognized as a realizable finite impulse response (FIR) filters system. Recently, the wavelet transform (WT) has been considered as a powerful tool for nonstationary signal analysis [1], [3], [7], [12], [16]. In [6] and [18], the fractional Brownian motion (fBm) process could be stationarized. Tewfik [18] and Kaplan [8] further proposed that the correlation function of a one-dimensional (1-D) fBm process decays hyperbolically at a rate determined by the number of vanishing moments of the wavelet function. However, all of these approaches mentioned above are suitable only for 1-D stochastic processes. The stationarization of multidimensional signals is seldom discussed. Because an image is considered as a 2-D signal generally, the generally used 1-D WT is necessarily extended to 2-D. Mallat [12] proposed a mathematical tool, called separable multiresolution subband filter, to adopt wavelet basis applied in image analysis.

This work will present theoretically that a nonstationary 2-D random field with wide-sense stationary increments/jumps (WSSI/WSSJ) can be stationarized by using a separable PR-QMF structure of 2-D DWT. The results apply to a sampled 2-D fBm field and a random field with WSSJ as the testbed. Furthermore, we will explore the decorrelation characteristic within the correlation functions of three detail images occurred in a 2-D fBm process. The decorrelation defined in [18] means that the correlation functions of the 2-D DWT images decay at a rate much faster than that of the fBm itself. These correlation functions are shown to decay at the order of  $H - \frac{L}{2}$  at

Manuscript received March 28, 1996; revised October 20, 1997. This work was supported by the National Science Council under Grant NSC85-2213-E-009-008. The associate editor coordinating the review of this manuscript and approving it for publication was Prof. C.-C. Jay Kuo.

The authors are with the Department of Electrical and Control Engineering, National Chiao Tung University, Hsinchu 300, Taiwan, R.O.C. (e-mail: bwu@haeshiuh.cn.nctu.edu.tw; su470219@ms1.hinet.net).

Publisher Item Identifier S 1057-7149(98)06391-X.

least on the basis for squares of the Euclidean distance of translations, where  $H$  denotes the parameter of the fBm and  $L$  is the vanishing moment of the wavelet function. Therefore, these three detail images behave much more like white as the parameter of fBm,  $H$ , goes down.

In Section II, we summarize the definitions of WSSI, WSSJ and wide-sense cyclostationary (WSCS) of a 2-D random field. The main results are developed in Section III. Section IV contains two examples to demonstrate the stationarization of the fields of WSSI and WSSJ. The conclusion is given in Section VI.

### II. PRELIMINARY

A mathematical tool proposed by Mallat [12] using wavelet basis to image analysis is extracted herein. Some properties of 2-D random fields [17, pp. 38–39] are reviewed here.

**Definition 1:** A 2-D random field  $\mathbf{f}[n_x, n_y]$  has WSSI's if the second moment of the increment,  $R_f[n_x1, n_y1; n_x2, n_y2; \tau_x2, \tau_y2] \equiv \mathcal{E}\{(\mathbf{f}[n_x1 + \tau_x1, n_y1 + \tau_y1] - \mathbf{f}[n_x1, n_y1]) (\mathbf{f}[n_x2 + \tau_x2, n_y2 + \tau_y2] - \mathbf{f}[n_x2, n_y2])\}$ , depends on  $n_x1, n_y1, n_x2$  and  $n_y2$  only through  $n_x1 - n_x2$  and  $n_y1 - n_y2$ ; i.e.,  $R_f[n_x1, n_y1; \tau_x1, \tau_y1; n_x2, n_y2; \tau_x2, \tau_y2] = R_f[n_x1 - n_x2, n_y1 - n_y2, \tau_x1, \tau_y1; 0, 0, \tau_x2, \tau_y2]$ ,  $\forall n_x1, n_y1, n_x2, n_y2, \tau_x1, \tau_y1, \tau_x2, \tau_y2 \in \mathbf{Z}$ , where  $\bar{\mathbf{f}}$  denotes the complex conjugate of  $\mathbf{f}$ .

**Definition 2:** A 2-D random field  $\mathbf{f}[n_x, n_y]$  is a process with WSSJ's if  $(\mathbf{f}[n_x + \tau_x, n_y + \tau_y] + \mathbf{f}[n_x, n_y])$  is wide-sense stationary (WSS),  $\forall n_x, n_y, \tau_x$  and  $\tau_y \in \mathbf{Z}$ .

**Definition 3:** A 2-D random field  $\mathbf{f}[n_x, n_y]$  is called WSCS with period  $T$  if  $\mathcal{E}\{\mathbf{f}[n_x + rT, n_y + rT]\} = \mathcal{E}\{\mathbf{f}[n_x, n_y]\}$  and  $R_f[(n_x1 + rT, n_y1 + rT), (n_x2 + rT, n_y2 + rT)] = R_f[(n_x1, n_y1), (n_x2, n_y2)]$ , for every integer  $r$ .

The above definitions are directly extended from the 1-D case in Papoulis [13, p. 373].

### III. MAIN RESULTS

Since image files are finite fields as usual, the length of an original 2-D random field  $f$  is set to be  $N \times N$  such that the approximate image  $A_m f$  and three detail images  $D_m^H f$ ,  $D_m^V f$ , and  $D_m^D f$  from [12] can be reduced to be

$$\begin{aligned} A_m f[k_x, k_y] &= \sum_{n_x=0}^{(N/2^{m-1})-1} \sum_{n_y=0}^{(N/2^{m-1})-1} h[(n_x - 2k_x) \frac{N}{2^{m-1}}] \\ &\quad \times h[(n_y - 2k_y) \frac{N}{2^{m-1}}] A_{m-1} f[n_x, n_y] \\ D_m^H f[k_x, k_y] &= \sum_{n_x=0}^{(N/2^{m-1})-1} \sum_{n_y=0}^{(N/2^{m-1})-1} h[(n_x - 2k_x) \frac{N}{2^{m-1}}] \\ &\quad \times g[(n_y - 2k_y) \frac{N}{2^{m-1}}] A_{m-1} f[n_x, n_y] \end{aligned}$$

and so forth, for  $D_m^V f$  and  $D_m^D f$ , where  $(n)_N$  denotes  $(n \text{ modulo } N)$ . Let  $\mathbf{F}$ ,  $\mathbf{A}_m$ , and  $\mathbf{D}_m^\varpi$  denote the following matrices of random fields, respectively:

$$\mathbf{F} \equiv [f[n_x, n_y]]_{N \times N}, \quad \mathbf{A}_m \equiv [A_m f[k_x, k_y]]_{\frac{N}{2^m} \times \frac{N}{2^m}}$$

and

$$\mathbf{D}_m^\varpi \equiv [D_m^\varpi f[k_x, k_y]]_{\frac{N}{2^m} \times \frac{N}{2^m}} \quad (1)$$

where  $\varpi = \mathbf{H}, \mathbf{V}$ , or  $\mathbf{D}$ , respectively,  $n_x, n_y = 0, 1, \dots, N-1$ , and  $k_x, k_y = 0, 1, \dots, \frac{N}{2^m} - 1$ . The linear operators  $\mathbf{H}_{m-1}$  and  $\mathbf{G}_{m-1}$

TABLE I  
AUTOCORRELATION DATA OF THE APPROXIMATE IMAGE,  $A_m f$ , AND THREE DETAIL IMAGES,  
 $D_m^d f$ ,  $d = H, V$  OR  $D$ , WITH  $m = 1$  FOR THE 2-D RANDOM FIELD WITH WSSI IN EXAMPLE 1

$m$	Autocorrelation	$\{(k_{x1}, k_{y1}), (k_{x2}, k_{y2})\}$	$H = 0.3$	$H = 0.5$	$H = 0.8$
			$\mathcal{E}\{xy^*\}$	$\mathcal{E}\{xy^*\}$	$\mathcal{E}\{xy^*\}$
1	$R_{D^H}$	$[(0, 0), (0, 0)]$	$4.5045e - 09$	$1.3132e - 09$	$2.7292e - 10$
		$[(1, 1), (1, 1)]$	$4.0157e - 09$	$1.1341e - 09$	$2.3067e - 10$
		$[(1, 2), (1, 2)]$	$4.3042e - 09$	$1.2236e - 09$	$2.4744e - 10$
1	$R_{D^V}$	$[(0, 0), (0, 0)]$	$3.9924e - 09$	$1.1474e - 09$	$2.4182e - 10$
		$[(1, 1), (1, 1)]$	$4.3307e - 09$	$1.2547e - 09$	$2.6422e - 10$
		$[(1, 2), (1, 2)]$	$4.4229e - 09$	$1.2758e - 09$	$2.6420e - 10$
1	$R_{D^D}$	$[(0, 0), (0, 0)]$	$1.5632e - 09$	$3.2238e - 10$	$3.1743e - 11$
		$[(1, 1), (1, 1)]$	$1.5850e - 09$	$3.2985e - 10$	$3.3107e - 11$
		$[(1, 2), (1, 2)]$	$1.5424e - 09$	$3.1958e - 10$	$3.1652e - 11$

1.  $\mathcal{E}\{xy^*\}$  denotes  $\mathcal{E}\{W_m f[k_{x1}, k_{y1}]W_m f^*[k_{x2}, k_{y2}]\}$ ,  $W = A, D^H, D^V$  or  $D^D$ .

2.  $\{B[n_x, n_y]\}$  is a  $128 \times 128$  sampled 2D fBm random field.

are two  $\frac{N}{2^m} \times \frac{N}{2^{m-1}}$  matrices,  $m \geq 1$ , whose entries are defined as

$$[H_{m-1}]_{k,i} \equiv h[i - 2k] \quad \text{and} \quad [G_{m-1}]_{k,i} \equiv g[i - 2k], \quad (2)$$

and satisfy

$$[H_{m-1}]_{k,i} = [H_{m-1}]_{k+1,i+2}$$

and

$$[G_{m-1}]_{k,i} = [G_{m-1}]_{k+1,i+2} \quad (3)$$

where  $i = 0, 1, \dots, \frac{N}{2^{m-1}} - 1$ ,  $k = 0, 1, \dots, \frac{N}{2^m} - 1$  and the additions  $k+1$  and  $i+2$  are, respectively, modulo  $\frac{N}{2^m}$  and  $\frac{N}{2^{m-1}}$ . According to the finite length of the 2-D random field, those wavelet images at  $m$ th resolution as defined in [12] can be formed into  $\frac{N}{2^m} \times \frac{N}{2^m}$  matrices for  $k_x, k_y = 0, 1, \dots, \frac{N}{2^m} - 1$  and all positive integers  $m < \log_2 N$ , which are expressed as

$$\begin{aligned} \mathbf{A}_m &= \mathbf{H}_{m-1} \mathbf{A}_{m-1} \mathbf{H}_{m-1}^T \\ &= \mathbf{H}_{m-1} \mathbf{H}_{m-2} \cdots \mathbf{H}_0 \mathbf{F} \mathbf{H}_0^T \cdots \mathbf{H}_{m-2}^T \mathbf{H}_{m-1}^T \end{aligned} \quad (4)$$

$$\begin{aligned} \mathbf{D}_m^H &= \mathbf{H}_{m-1} \mathbf{A}_{m-1} \mathbf{G}_{m-1}^T \\ &= \mathbf{H}_{m-1} \mathbf{H}_{m-2} \cdots \mathbf{H}_0 \mathbf{F} \mathbf{H}_0^T \cdots \mathbf{H}_{m-2}^T \mathbf{G}_{m-1}^T \end{aligned} \quad (5)$$

$$\begin{aligned} \mathbf{D}_m^V &= \mathbf{G}_{m-1} \mathbf{A}_{m-1} \mathbf{H}_{m-1}^T \\ &= \mathbf{G}_{m-1} \mathbf{H}_{m-2} \cdots \mathbf{H}_0 \mathbf{F} \mathbf{H}_0^T \cdots \mathbf{H}_{m-2}^T \mathbf{H}_{m-1}^T \end{aligned} \quad (6)$$

and

$$\begin{aligned} \mathbf{D}_m^D &= \mathbf{G}_{m-1} \mathbf{A}_{m-1} \mathbf{G}_{m-1}^T \\ &= \mathbf{G}_{m-1} \mathbf{H}_{m-2} \cdots \mathbf{H}_0 \mathbf{F} \mathbf{H}_0^T \cdots \mathbf{H}_{m-2}^T \mathbf{G}_{m-1}^T \end{aligned} \quad (7)$$

where the superscript  $T$  indicates the notation of transposition. In this framework, the reconstruction formula in [12] can be written as

$$\begin{aligned} \mathbf{A}_{m-1} &= \mathbf{H}_{m-1}^T \mathbf{A}_m \mathbf{H}_{m-1} + \mathbf{H}_{m-1}^T \mathbf{D}_m^H \mathbf{G}_{m-1} \\ &\quad + \mathbf{G}_{m-1}^T \mathbf{D}_m^V \mathbf{H}_{m-1} + \mathbf{G}_{m-1}^T \mathbf{D}_m^D \mathbf{G}_{m-1}. \end{aligned} \quad (8)$$

The right Kronecker (or direct) product  $\mathbf{A} \otimes \mathbf{B}$  of two  $\frac{N}{2^m} \times \frac{N}{2^{m-1}}$  matrices,  $[a_{i,j}]$  and  $[b_{i,j}]$ , is defined as [11, p. 407]

$$\begin{aligned} \Theta_{AB, m-1} &\equiv \mathbf{A} \otimes \mathbf{B} \\ &= \begin{bmatrix} a_{0,0} \mathbf{B} & a_{0,1} \mathbf{B} & \cdots & a_{0, \frac{N}{2^{m-1}} - 1} \mathbf{B} \\ a_{1,0} \mathbf{B} & a_{1,1} \mathbf{B} & \cdots & a_{1, \frac{N}{2^{m-1}} - 1} \mathbf{B} \\ \vdots & \vdots & \ddots & \vdots \\ a_{\frac{N}{2^m} - 1, 0} \mathbf{B} & a_{\frac{N}{2^m} - 1, 1} \mathbf{B} & \cdots & a_{\frac{N}{2^m} - 1, \frac{N}{2^{m-1}} - 1} \mathbf{B} \end{bmatrix}. \end{aligned} \quad (9)$$

From (3), it yields that the elements of  $\Theta_{AB, m-1}$  have the following relationship: 1

$$\begin{aligned} [\Theta_{AB, m-1}]_{i+l, \frac{N}{2^m}, j+k, \frac{N}{2^{m-1}}} &= [\Theta_{AB, m-1}]_{i+l, \frac{N}{2^m}, j+k, \frac{N}{2^{m-1}} + 2} \\ &= [\Theta_{AB, m-1}]_{i+(l+1), \frac{N}{2^m}, j+(k+2), \frac{N}{2^{m-1}}} \end{aligned} \quad (10)$$

for  $m \geq 1$ ,  $i, l = 0, 1, \dots, \frac{N}{2^m} - 1$ , and  $j, k = 0, 1, \dots, \frac{N}{2^{m-1}} - 1$ , where  $\mathbf{A}$  and  $\mathbf{B}$  denote  $\mathbf{H}_{m-1}$  or  $\mathbf{G}_{m-1}$ . For the convenience of manipulation as the following, we assume that  $\Theta_{AB, m-1}$  is in period in both the row and column blocks (or elements in each block) with period  $\frac{N}{2^m}$  and  $\frac{N}{2^{m-1}}$ , respectively.

Now, let a column vector be generated by column-scanning the random matrix  $\mathbf{F}$ , called the *vec-function* of  $\mathbf{F}$ , which is denoted as  $\text{vec } \mathbf{F}$  or  $\vec{F}$ . It is concatenated with one column followed by another as shown below:

$$\text{vec } \mathbf{F} \equiv [f[0, 0] \quad f[1, 0] \quad \cdots \quad f[N-1, 0] \quad f[0, 1] \quad \cdots \quad f[N-1, 1] \quad \cdots \quad f[N-1, N-1]]^T \quad (11)$$

which is an  $N^2$ -dimensional vector. Let  $\mathbf{R}_{\vec{F}} \equiv \mathcal{E}\{(\text{vec } \mathbf{F})(\text{vec } \mathbf{F})^*\}$  be the autocorrelation matrix of  $\text{vec } \mathbf{F}$  where the superscript  $*$

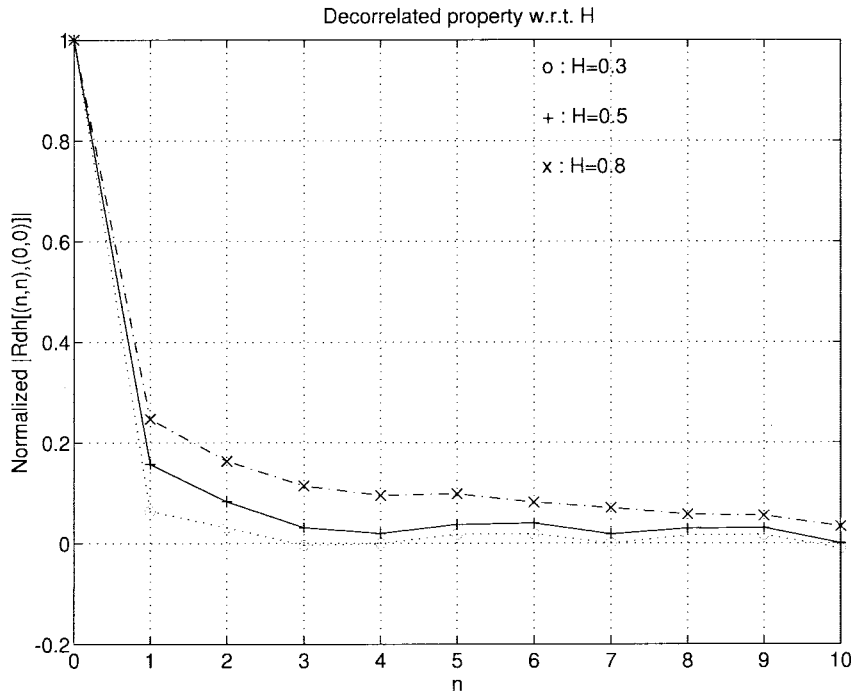


Fig. 1. Profiles of  $R_{DH}$  of the 2-D fBm field w.r.t.  $H = 0.3$ ,  $H = 0.5$  and  $H = 0.8$  for  $m = 1$  in Example 1, where “o”:  $H = 0.3$ , “+”:  $H = 0.5$ , “x”:  $H = 0.8$ .

indicates the notation of complex conjugate and transposition. Define  $\mathbf{R}_{\tilde{\mathbf{A}}_m}$  as the autocorrelation matrix of  $\text{vec } \mathbf{A}_m$ , and so forth, for  $\mathbf{R}_{\tilde{\mathbf{D}}_m^\varpi}$ , where  $\varpi$  denotes  $\mathbf{H}$ ,  $\mathbf{V}$  or  $\mathbf{D}$ . The cross-correlation matrix of  $\text{vec } \mathbf{A}_m$  and  $\text{vec } \mathbf{D}_m^\varpi$  is also defined as  $\mathbf{R}_{\tilde{\mathbf{A}}_m \tilde{\mathbf{D}}_m^\varpi} \equiv \mathcal{E}\{(\text{vec } \mathbf{A}_m)(\text{vec } \mathbf{D}_m^\varpi)^*\}$  and so forth for  $\mathbf{R}_{\tilde{\mathbf{D}}_m^\varpi \tilde{\mathbf{D}}_m^\beta}$ , where  $\varpi$  and  $\beta = \mathbf{H}, \mathbf{V}$  or  $\mathbf{D}$ .

The main result is concluded in the following stationarization theorem, called *2-D stationarization theorem* (2-D ST). And the 2-D DWT images related to a 2-D fBm process is shown to have the decorrelation characteristics.

**Theorem 1 (2-D Stationarization Theorem):** Let  $\mathbf{f}[n_x, n_y]$ ,  $n_x$  and  $n_y = 0, 1, \dots, N-1$ , be a 2-D real random field with constant mean and autocorrelation function  $R_f[(n_{x1}, n_{y1}), (n_{x2}, n_{y2})] \equiv \mathcal{E}\{\mathbf{f}[n_{x1}, n_{y1}] \overline{\mathbf{f}[n_{x2}, n_{y2}]}\}$ . Let  $\mathbf{f}[n_x, n_y]$  be decomposed into one approximate image,  $A_m f$ , and three detail images,  $D_m^H f$ ,  $D_m^V f$ , and  $D_m^D f$ , as described in [12]. If  $\mathbf{f}[n_x, n_y]$  satisfies the condition,

$$(C): \frac{R_f[(n_{x1}, n_{y1}), (n_{x2}, n_{y2})]}{(1+n_{x1}^2+n_{y1}^2+n_{x2}^2+n_{y2}^2)^{N_R}} \in l^\infty, \text{ for some } N_R > 0, \\ N_R \in \mathbf{Z} \text{ and } \forall n_{x1}, n_{y1}, n_{x2}, n_{y2} \in \mathbf{Z}, \text{ then, for any positive integer } m < \log_2 N, \text{ we obtain that}$$

- (P1): if  $\mathbf{f}[n_x, n_y]$  is WSS, then  $A_m f$ ,  $D_m^H f$ ,  $D_m^V f$ , and  $D_m^D f$  are WSS, respectively, and jointly each other for all  $n_x$  and  $n_y$ , i.e.,  $\mathbf{R}_{\tilde{\mathbf{A}}_m}$ ,  $\mathbf{R}_{\tilde{\mathbf{D}}_m^\varpi}$ ,  $\mathbf{R}_{\tilde{\mathbf{A}}_m \tilde{\mathbf{D}}_m^\varpi}$ , and  $\mathbf{R}_{\tilde{\mathbf{D}}_m^\varpi \tilde{\mathbf{D}}_m^\beta}$  are Hermitian block Toeplitz matrix with Toeplitz blocks, where  $\varpi$  and  $\beta = \mathbf{H}, \mathbf{V}$  or  $\mathbf{D}$ , respectively;
- (P2): if  $\mathbf{f}[n_x, n_y]$  has WSSI, then  $D_m^H f$ ,  $D_m^V f$  and  $D_m^D f$  are WSS, respectively, and jointly each other for all  $n_x$  and  $n_y$ , i.e.,  $\mathbf{R}_{\tilde{\mathbf{D}}_m^\varpi}$  and  $\mathbf{R}_{\tilde{\mathbf{D}}_m^\varpi \tilde{\mathbf{D}}_m^\beta}$  are Hermitian block Toeplitz matrix with Toeplitz blocks where  $\varpi$  and  $\beta = \mathbf{H}, \mathbf{V}$  or  $\mathbf{D}$ , respectively; moreover,
- (P3): if  $A_m f$ ,  $D_m^H f$ ,  $D_m^V f$ , and  $D_m^D f$  are WSS, respectively, and jointly each other for all  $n_x$  and  $n_y \in \mathbf{Z}$ , then  $\mathbf{f}[n_x, n_y]$  is WSCS with period 2, i.e.,

$$[\mathbf{R}_{\tilde{\mathbf{f}}}]_{i,j} = [\mathbf{R}_{\tilde{\mathbf{f}}}]_{i+2,j+2}; \quad (12)$$

(J): if  $\mathbf{f}[n_x, n_y]$  is a process with WSSJ, then three detail images,  $D_m^H f$ ,  $D_m^V f$ , and  $D_m^D f$ , are WSS, respectively, and jointly for all  $n_x, n_y \in \mathbf{Z}$ .

*Proof:* See Appendix A.  $\square$

#### A. 2-D fBm Field

The fBm process, as a well-known nonstationary stochastic process with WSSI having statistical properties and the modelings of image texture, has been discussed in many literatures. Tewfik [18] and Kaplan [8] proposed that the correlation functions of the 1-D DWT decay at a rate much faster than the correlation functions of the 1-D fBm itself. In this correspondence, we will show that the 2-D DWT based on PR-QMF structure is also capable of preserving the property for a 2-D fBm field.

Consider a zero-mean sampled 2-D fBm random field,  $B[n_x, n_y] \equiv B_H(n_x \Delta x, n_y \Delta y)$ ,  $\forall n_x, n_y \in \mathbf{Z}$ , where  $\Delta x$  and  $\Delta y$  are the sampling periods of  $x, y$  directions, respectively, and the autocorrelation function of the 2-D fBm field is qualified to condition (C) in 2-D ST derived from [5, p. 250].

**Theorem 2:** Suppose that a wavelet function has the vanishing moment  $L$ . Then the autocorrelation functions of the horizontal and vertical detail images related to a 2-D fBm random field  $B[n_x, n_y]$ , denoted as  $D_m^H B$  and  $D_m^V B$ , respectively, decay as  $\mathcal{O}((\tau_x^2 + \tau_y^2)^{H-\nu})$  with  $\nu \geq \frac{L}{2}$ , where  $\tau_x \equiv n_{x1} - n_{x2}$  and  $\tau_y \equiv n_{y1} - n_{y2}$ , for all  $n_{x1}, n_{x2}, n_{y1}$  and  $n_{y2} \in \mathbf{Z}$ . Furthermore, for the diagonal detail image, denoted as  $D_m^D B$ , the autocorrelation function decays with the order of  $H - \nu, \nu \geq L$ .

*Proof:* See Appendix B.  $\square$

**Remark 1:** Three detail images of a 2-D fBm random field  $B[n_x, n_y]$  are WSS with the corresponding autocorrelation functions are symmetric with respect to (w.r.t.) the axes'  $\tau_x$  and  $\tau_y$ . Therefore,  $D_m^H B$ ,  $D_m^V B$  and  $D_m^D B$  are approximated to be white for any positive integer  $m$  as the vanishing moment  $L > 1$  for  $D_m^D$  and  $L > 2$  for  $D_m^H$  and  $D_m^V$ . The decay is too slow when  $H > 0.5$ .

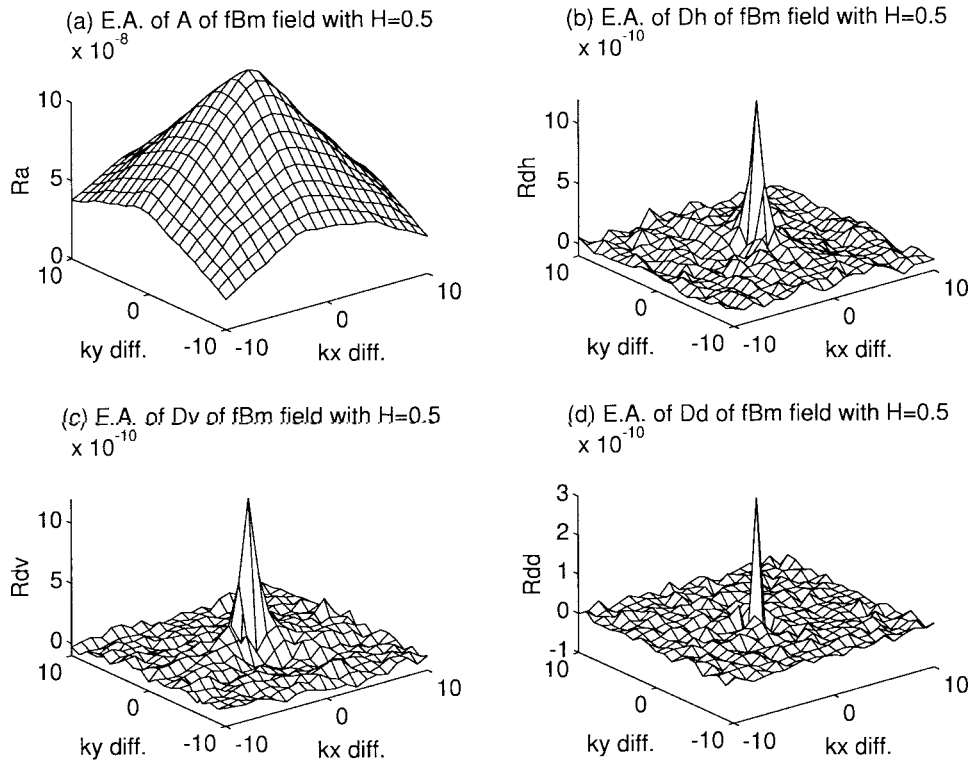


Fig. 2. Autocorrelation functions of the 2-D DWT images of the 2-D fBm (WSSI) field with parameter  $H = 0.5$  for the case of  $m = 1$  in Example 1, (a)  $R_A[(10, 10), (k_{x2}, k_{y2})]$ , (b)  $R_{DH}[(10, 10), (k_{x2}, k_{y2})]$ , (c)  $R_{DV}[(10, 10), (k_{x2}, k_{y2})]$ , (d)  $R_{DD}[(10, 10), (k_{x2}, k_{y2})]$ , where  $k_x \text{ diff} \equiv k_{x2} - 10$  and  $k_y \text{ diff} \equiv k_{y2} - 10$ .

From Theorem 2 and Remark 1, it yields that the three detail images of a 2-D fBm random field behave much more like white noises as the parameter  $H$  becomes smaller.

#### IV. EXAMPLES

The sampled 2-D fBm field generated by the spectral synthesis method [14, pp. 96–105] is used in Example 1 to present the case (P2) of 2-D ST and the result derived in Remark 1. The spectral synthesis method is an approximate method, but it does not affect the validity of our illustration. In the second example, a 2-D autoregressive integrated moving average (ARIMA) model extended from a 1-D ARIMA model in [10] is used to generate the 2-D random field with WSSJ to demonstrate the case (J) of 2-DST.

*Example 1 (The WSSI Field):* Take a sampled 2-D fBm random field denoted by  $B[n_x, n_y]$ ,  $n_x, n_y = 0, 1, \dots, 127$ , for  $H = 0.3$ ,  $H = 0.5$  and  $H = 0.8$  cases, and choose the Haar basis for simplicity, i.e.,  $h[0] = h[1] = g[0] = -g[1] = \frac{1}{\sqrt{2}}$ , with 1280 Monte-Carlo runs. The stationary property of three detail images is shown in Table I which demonstrates the results derived from Theorem 1. From Fig. 1, we obtain that the ensemble-averaging correlation functions of  $R_{DH}$  decay fast when the parameter  $H$  decreases. The more  $H$  get close zero, the more 2-D DWT of the fBm approach white. The phenomenon in Fig. 2(a) shows that the approximate image decays much slower than three detail images. In Fig. 2(b)–(d), the autocorrelation functions of three detail images are symmetric w.r.t. the axes of  $k_{x2}$  and  $k_{y2}$  around the center  $(10, 10)$ , but not isotropic. It is corresponding to the result derived in Remark 1.

*Example 2 (The WSSJ Field):* Consider a nonstationary 2-D random field  $\{f[n_x, n_y]\}_{n_x, n_y=0, 1, \dots, 255}$  given by

$$f[n_x, n_y] + f[n_x + 1, n_y + 1] = \nu[n_x, n_y] \quad (13)$$

where  $\{\nu[n_x, n_y]\}_{n_x, n_y \in \mathbb{Z}}$  is an i.i.d. normal distribution with mean zero and variance 1. Obviously, the jump's field is a white noise field as designed. The simulation is based on 1000 Monte-Carlo runs with the Haar basis. The contour maps of the autocorrelation functions for the approximate image and three detail images of  $f$  at two different time ranges  $[(64, 64), (k_{x2}, k_{y2})]$ ,  $k_{x2}k_{y2} = 54 \sim 74$ , and  $[(74, 74), (k_{x2}, k_{y2})]$ ,  $k_{x2}, k_{y2} = 64 \sim 84$ , are drawn with 7 contour lines in Figs. 3 and 4, respectively. Comparatively, both the autocorrelation functions of the approximate and three detail images are proven clearly to be stationary conformable to the conclusion of the case (J) in 2-D ST.

#### V. CONCLUSION

It has been shown that a 2-D DWT performed on separable PR-QMF structure could provide the stationarizability property for a nonstationary 2-D random field with WSSI/WSSJ, and the decay rates of the correlation functions of three detail images for a 2-D fBm field are dependent upon the parameter of the fBm,  $H$ . These correlation functions are proven to decay with the order of  $H - \frac{L}{2}$  ( $H - L$  for the diagonal detail image) based on the squares of the distance of translations. From the results of simulation in conformity with 2-D ST in this work, we observed that the correlation functions of three detail images for the 2-D fBm are invariant and symmetric along  $k_{x1} - k_{x2}$  and  $k_{y1} - k_{y2}$ , but not stationary along the distance,  $\sqrt{(k_{x1} - k_{x2})^2 + (k_{y1} - k_{y2})^2}$ .

#### APPENDIX A

##### PROOF OF THEOREM 1: 2-D STATIONARIZATION THEOREM

The proof of (P1) (i.e., for the case of WSS) could be obtained easily by similar but simpler procedures as the following proof of (P2).

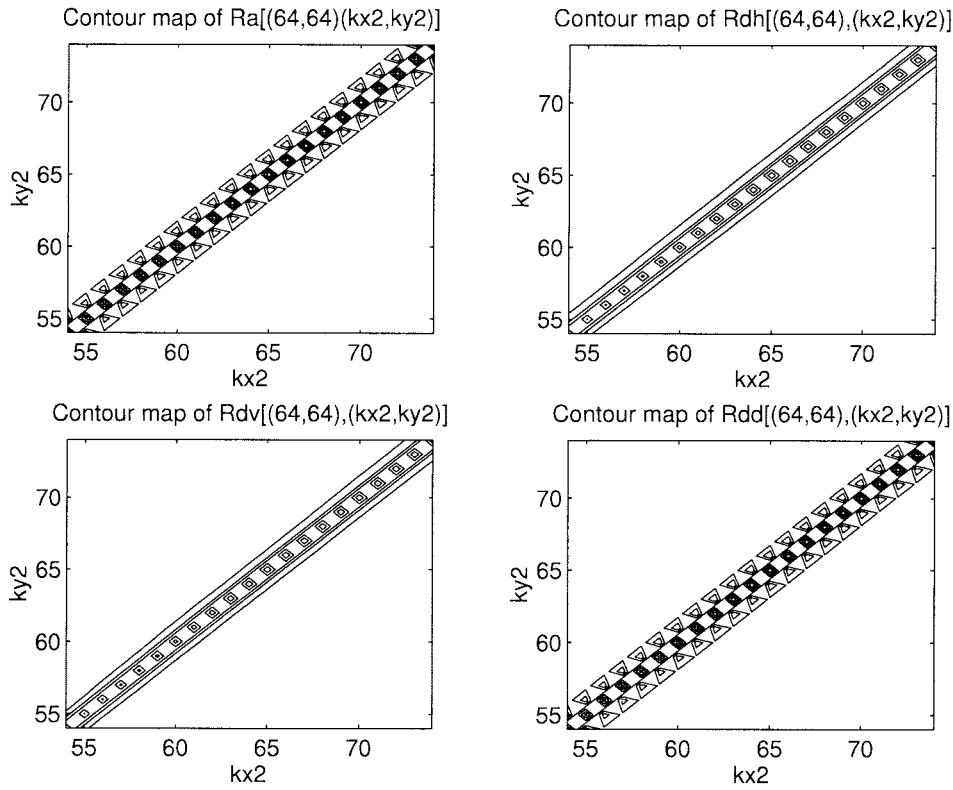


Fig. 3. Contour maps of the autocorrelation functions for the approximate image and three detail images of the WSSJ field at the range  $[(64, 64), (k_{x2}, k_{y2})]$ , where  $k_{x2} : 54 \sim 74$  and  $k_{y2} : 54 \sim 74$ , in Example 2.

*Proof of (P2):* If  $\mathbf{f}[n_x, n_y]$  has WSSI, the properties of constant means for three detail images,  $D_m^H f$ ,  $D_m^V f$  and  $D_m^D f$ , are qualified straight for any positive integer  $m$ . The procedures to prove the stationarity of the second order statistics for the three detail images are similar, therefore, we only take  $D_m^H f$  to be shown thoroughly in the following:

i) For any positive integer  $m$ , the autocorrelation function of  $D_m^H f$  is shown easily to be bounded.

ii) Since the real process  $\mathbf{f}$  is of WSSI, define  $\mathbf{y}_{\vec{r}}[\vec{n}] \equiv \mathbf{f}[\vec{n}] - \mathbf{f}[\vec{n} - \vec{r}]$ ,  $\vec{n} \equiv [n_x, n_y]$ , for every integer vector  $\vec{r} \equiv [r_x, r_y]$ ,  $n_x, n_y, r_x, r_y = 0, 1, \dots, N-1$ . Followingly, choose any integer vector  $\vec{r} \equiv [r_x, r_y]$ . Let  $\vec{s} = -\vec{r} \equiv [s_x, s_y]$  such that  $\vec{r} = \vec{n}_1 - \vec{l}_1$ ,  $\vec{s} = \vec{l}_1 - \vec{n}_1$ , and the correlation function between  $\mathbf{y}_{\vec{r}}[\vec{n}_1] \equiv \mathbf{y}_{\vec{r}}[n_{x1}, n_{y1}]$  and  $\mathbf{y}_{\vec{s}}[\vec{l}_1] \equiv \mathbf{y}_{\vec{s}}[l_{x1}, l_{y1}]$  is stationary and satisfies

$$\begin{aligned} R_{y_{\vec{r}}y_{\vec{s}}}[\vec{n}_1, \vec{l}_1] &\equiv \mathcal{E}\{\mathbf{y}_{\vec{r}}[\vec{n}_1]\mathbf{y}_{\vec{s}}[\vec{l}_1]\} = R_f[\vec{n}_1, \vec{l}_1] \\ &\quad - R_f[\vec{n}_1, \vec{n}_1] - R_f[\vec{l}_1, \vec{l}_1] + R_f[\vec{l}_1, \vec{n}_1], \\ &= \mathcal{E}\{|\vec{n}_1 - \vec{l}_1|^2\} = d_1(|\vec{n}_1 - \vec{l}_1|) \end{aligned} \quad (\text{A1})$$

where  $d_1(\cdot)$  is function of  $\vec{r}$  due to the stationarity of  $\mathbf{y}_{\vec{r}}$  and  $\mathbf{y}_{\vec{s}}$ . In the literature, the function  $d_1(\cdot)$  is known as the structure function [19, pp. 391–394]. Based on one vanishing moment of  $g$ , (10) and the result of (P1), we therefore obtain that the horizontal detail image of  $\mathbf{y}_{\vec{r}}$  defined as

$$\begin{aligned} D_m^H(\mathbf{y}_{\vec{r}})[k_{x1}, k_{y1}] & \\ \equiv \sum_{n_{xm}=0}^{\frac{N}{2^{m-1}}-1} \sum_{n_{ym}=0}^{\frac{N}{2^{m-1}}-1} \cdots \sum_{n_{y1}=0}^{N-1} & h[(n_{xm} - 2k_{xm-1})\frac{N}{2^{m-1}}] \\ \times g[(n_{ym} - 2k_{ym-1})\frac{N}{2^{m-1}}] \cdots & h[(n_{y1} - 2n_{y2})_N] \mathbf{y}_{\vec{r}}[n_{x1}, n_{y1}] \end{aligned}$$

is stationary, and the correlation function of  $D_m^H(f)$  for all  $k_{x1}, k_{y1}, k_{x2}, k_{y2} \in \mathbf{Z}$  is given by

$$\begin{aligned} R_{D_m^H(f)}[(k_{x1}, k_{y1}), (k_{x2}, k_{y2})] & \\ \equiv \mathcal{E}_f\{D_m^H f[k_{x1}, k_{y1}]\overline{D_m^H f[k_{x2}, k_{y2}]}\} & \\ = \sum_{n_{xm}=0}^{\frac{N}{2^{m-1}}-1} \sum_{n_{ym}=0}^{\frac{N}{2^{m-1}}-1} \cdots \sum_{n_{y1}=0}^{N-1} \sum_{l_{xm}=0}^{\frac{N}{2^{m-1}}-1} \sum_{l_{ym}=0}^{\frac{N}{2^{m-1}}-1} \cdots \sum_{l_{y1}=0}^{N-1} & \\ \times h[(n_{xm} - 2k_{x1})\frac{N}{2^{m-1}}] g[(n_{ym} - 2k_{y1})\frac{N}{2^{m-1}}] \cdots & \\ \overline{g[(l_{ym} - 2k_{y2})\frac{N}{2^{m-1}}]} \cdots \overline{h[(l_{y1} - 2l_{y2})_N]} & \\ \times R_f[(n_{x1}, n_{y1}), (l_{x1}, l_{y1})], & \\ = \sum_{n_{xm}=0}^{\frac{N}{2^{m-1}}-1} \sum_{n_{ym}=0}^{\frac{N}{2^{m-1}}-1} \cdots \sum_{n_{y1}=0}^{N-1} \sum_{l_{xm}=0}^{\frac{N}{2^{m-1}}-1} \sum_{l_{ym}=0}^{\frac{N}{2^{m-1}}-1} \cdots \sum_{l_{y1}=0}^{N-1} & \\ \times h[(n_{xm} - 2k_{x1})\frac{N}{2^{m-1}}] g[(n_{ym} - 2k_{y1})\frac{N}{2^{m-1}}] \cdots & \\ \overline{g[(l_{ym} - 2k_{y2})\frac{N}{2^{m-1}}]} \cdots \overline{h[(l_{y1} - 2l_{y2})_N]} & \\ \times \frac{1}{2}\{R_{y_{\vec{r}}y_{\vec{s}}}[(n_{x1}, n_{y1}), (l_{x1}, l_{y1})] + R_f[(n_{x1}, n_{y1}), (n_{x1}, n_{y1})] & \\ + R_f[(l_{x1}, l_{y1}), (l_{x1}, l_{y1})]\}, & \\ = \sum_{n_{xm}=0}^{\frac{N}{2^{m-1}}-1} \sum_{n_{ym}=0}^{\frac{N}{2^{m-1}}-1} \cdots \sum_{n_{y1}=0}^{N-1} \sum_{l_{xm}=0}^{\frac{N}{2^{m-1}}-1} \sum_{l_{ym}=0}^{\frac{N}{2^{m-1}}-1} \cdots \sum_{l_{y1}=0}^{N-1} & \\ \times h[(n_{xm} - 2k_{x1})\frac{N}{2^{m-1}}] g[(n_{ym} - 2k_{y1})\frac{N}{2^{m-1}}] \cdots & \\ \overline{h[(l_{y1} - 2l_{y2})_N]} \frac{1}{2} R_{y_{\vec{r}}y_{\vec{s}}}[(n_{x1}, n_{y1}), (l_{x1}, l_{y1})] & \\ = \frac{1}{2} R_{D_m^H(y_{\vec{r}}y_{\vec{s}})}[(k_{x1}, k_{y1}), (k_{x2}, k_{y2})] & \end{aligned} \quad (\text{A2})$$

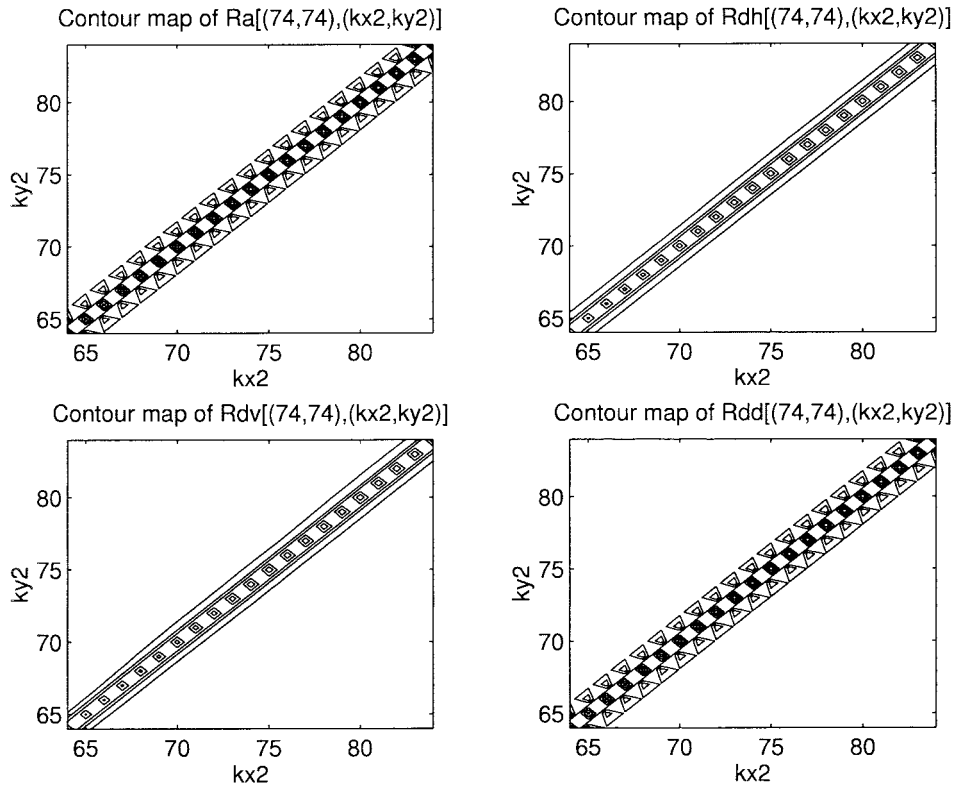


Fig. 4. Contour maps of the autocorrelation functions for the approximate image and three detail images of the WSSJ field at the range  $[(74, 74), (k_{x2}, k_{y2})]$ , where  $k_{x2} : 64 \sim 84$  and  $k_{y2} : 64 \sim 84$ , in Example 2.

where  $\bar{h}$  denotes the complex conjugate of  $h$ . Hence, (A2) can be described by the following matrix equation, such that the correlation matrix of  $\bar{\mathbf{D}}_m^H(f)$  is equivalent to one half of the correlation matrix  $\mathbf{R}_{\bar{\mathbf{D}}_m^H(y_{rx}y_s)}$  [11, p. 410].

$$\mathbf{R}_{\bar{\mathbf{D}}_m^H(f)} = \frac{1}{2} \mathbf{R}_{\bar{\mathbf{D}}_m^H(y_{rx}y_s)} = \frac{1}{2} \Theta_{GH,m-1} \Theta_{HH,m-2} \cdots \Theta_{HH,0} \Lambda \Theta_{HH,0}^* \cdots \Theta_{HH,m-2}^* \Theta_{GH,m-1}^*, \quad (\text{A3})$$

where the elements of matrix  $\Lambda$  are composed of the structure function evaluated at various lags, i.e.,

$$\Lambda \equiv [d_1(|\vec{n}_1 - \vec{l}_1|)]_{\vec{n}_1, \vec{l}_1 = (0,0), (1,0), \dots, (N-1,0), (0,1), \dots, (N-1,1), \dots, (N-1, N-1)},$$

$\Lambda$  is also a Hermitian Toeplitz matrix with Toeplitz blocks. Here, we assume that  $\Lambda$  is period in both the row and column blocks with period  $N$  and every block is also period in both the row and column elements with period  $N$ . Note that  $\Lambda$  is not positive definite, but  $\mathbf{R}_{\bar{\mathbf{D}}_m^H(f)}$  is positive definite.

The property of the Hermitian block Toeplitz matrix with Toeplitz blocks for  $\mathbf{R}_{\bar{\mathbf{D}}_m^H(f)}$  will be manipulated in the following processes for any positive integer  $m$ ,  $k_x = k_1 + l_1 \frac{N}{2^m}$ ,  $k_y = k_2 + l_2 \frac{N}{2^m}$ , where the indices inside each block are denoted as  $k_1, k_2 = 0, 1, \dots, \frac{N}{2^m} - 1$  and the indices of blocks are  $l_1, l_2 = 0, 1, \dots, \frac{N}{2^m} - 1$ , (a) for block matrix and any  $k_1, k_2$ :

$$\begin{aligned} & [\mathbf{R}_{\bar{\mathbf{D}}_m^H(f)}]_{l_1 \frac{N}{2^m} + k_1, l_2 \frac{N}{2^m} + k_2} \\ &= \frac{1}{2} \sum_{i_{m-1}=0}^{(\frac{N}{2^{m-1}})^2 - 1} \cdots \sum_{i_0=0}^{(N)^2 - 1} \sum_{j_0=0}^{(N)^2 - 1} \cdots \sum_{j_{m-1}=0}^{(\frac{N}{2^{m-1}})^2 - 1} \end{aligned}$$

$$\begin{aligned} & \times [\Theta_{GH,m-1}]_{l_1 \frac{N}{2^m} + k_1, i_{m-1} \frac{N}{2^{m-1}} + k_2} \cdots \\ & [\Theta_{HH,0}]_{i_1 \frac{N}{2} + k_2, i_0 + k_2} [\Lambda]_{i_0 N + k_2, j_0 N + k_2} \\ & \times [\Theta_{HH,0}^*]_{j_0 N + k_2, j_1 \frac{N}{2} + k_2} \cdots \\ & [\Theta_{GH,m-1}^*]_{j_{m-1} \frac{N}{2^{m-1}} + k_2, l_2 \frac{N}{2^m} + k_2} \\ &= \frac{1}{2} \sum_{i_{m-1}=0}^{(\frac{N}{2^{m-1}})^2 - 1} \cdots \sum_{i_0=0}^{(N)^2 - 1} \sum_{j_0=0}^{(N)^2 - 1} \cdots \sum_{j_{m-1}=0}^{(\frac{N}{2^{m-1}})^2 - 1} \\ & \times [\Theta_{GH,m-1}]_{(l_1+1) \frac{N}{2^m} + k_1, (i_{m-1}+2) \frac{N}{2^{m-1}} + k_2} \cdots \\ & [\Theta_{HH,0}]_{(i_1+2^{m-1}) \frac{N}{2} + k_2, (i_0+2^m) N + k_2} \\ & \times [\Lambda]_{(i_0+2^m) N + k_2, (j_0+2^m) N + k_2} \\ & \times [\Theta_{HH,0}^*]_{(j_0+2^m) N + k_2, (j_1+2^{m-1}) \frac{N}{2} + k_2} \cdots \\ & [\Theta_{GH,m-1}^*]_{(j_{m-1}+2) \frac{N}{2^{m-1}} + k_2, (l_2+1) \frac{N}{2^m} + k_2} \\ &= [\mathbf{R}_{\bar{\mathbf{D}}_m^H(f)}]_{(l_1+1) \frac{N}{2^m} + k_1, (l_2+1) \frac{N}{2^m} + k_2} \quad (\text{A4}) \end{aligned}$$

and (b) for inside block and any  $l_1, l_2$ :

$$\begin{aligned} & [\mathbf{R}_{\bar{\mathbf{D}}_m^H(f)}]_{l_1 \frac{N}{2^m} + k_1, l_2 \frac{N}{2^m} + k_2} \\ &= \frac{1}{2} \sum_{i_{m-1}=0}^{(\frac{N}{2^{m-1}})^2 - 1} \cdots \sum_{i_0=0}^{(N)^2 - 1} \sum_{j_0=0}^{(N)^2 - 1} \cdots \sum_{j_{m-1}=0}^{(\frac{N}{2^{m-1}})^2 - 1} \\ & \times [\Theta_{GH,m-1}]_{l_1 \frac{N}{2^m} + k_1, l_2 \frac{N}{2^m} + k_2} \cdots \\ & [\Theta_{HH,0}]_{l_2 \frac{N}{2} + i_1, l_2 N + i_0} [\Lambda]_{l_2 N + i_0, l_2 N + j_0} \\ & \times [\Theta_{HH,0}^*]_{l_2 N + j_0, l_2 \frac{N}{2} + j_1} \cdots [\Theta_{GH,m-1}^*]_{l_2 \frac{N}{2^{m-1}} + j_{m-1}, l_2 \frac{N}{2^m} + k_2} \\ &= \frac{1}{2} \sum_{i_{m-1}=0}^{(\frac{N}{2^{m-1}})^2 - 1} \cdots \sum_{i_0=0}^{(N)^2 - 1} \sum_{j_0=0}^{(N)^2 - 1} \cdots \sum_{j_{m-1}=0}^{(\frac{N}{2^{m-1}})^2 - 1} \end{aligned}$$

$$\begin{aligned}
& \times [\Theta_{\text{GH},m-1}]_{l_1 \frac{N}{2^m} + (k_1+1), l_2 \frac{N}{2^m-1} + (i_{m-1}+2)} \cdots \\
& [\Theta_{\text{HH},0}]_{l_2 \frac{N}{2} + (i_1+2^{m-1}), l_2 N + (i_0+2^m)} \\
& \times [\mathbf{A}]_{l_2 N + (i_0+2^m), l_2 N + (j_0+2^m)} \\
& \times [\Theta_{\text{HH},0}^*]_{l_2 N + (j_0+2^m), l_2 \frac{N}{2} + (j_1+2^{m-1})} \cdots \\
& [\Theta_{\text{GH},m-1}^*]_{l_2 \frac{N}{2^m-1} + (j_{m-1}+2), l_2 \frac{N}{2^m} + (k_2+1)} \\
= & [\mathbf{R}_{\text{DH}_m^{\text{H}}}(\mathbf{f})]_{l_1 \frac{N}{2^m} + (k_1+1), l_2 \frac{N}{2^m} + (k_2+1)}. \tag{A5}
\end{aligned}$$

Hence,  $\mathbf{R}_{\text{DH}_m^{\text{H}}}(\mathbf{f})$  is a Hermitian block Toeplitz matrix with Toeplitz blocks, i.e.,  $D_m^{\text{H}} \mathbf{f}$  is WSS.

The proofs of (P3) and (J) are similar to the proof of (P2).  $\square$

#### APPENDIX B PROOF OF THEOREM 2

The proof of  $D_m^{\text{H}} B$ ,  $D_m^{\text{V}} B$  and  $D_m^{\text{D}} B$  are resembling. Herein we only take one of them shown below in detail. Let  $\tau_x \equiv k_{x1} - k_{x2}$  and  $\tau_y \equiv k_{y1} - k_{y2}$ , for all  $k_{x1}$ ,  $k_{x2}$ ,  $k_{y1}$ ,  $k_{y2} \in \mathbf{Z}$ . The autocorrelation of  $D_m^{\text{H}}(B)$  is written as

$$\begin{aligned}
& R_{D_m^{\text{H}}(B)}[\tau_x, \tau_y] \\
& \equiv \mathcal{E}\{D_m^{\text{H}} B[k_{x1}, k_{y1}] \overline{D_m^{\text{H}} B[k_{x2}, k_{y2}]}\} \\
& = \sum_{i_1} \cdots \sum_{i_m} \sum_{l_1} \cdots \sum_{l_m} \sum_{j_1} \cdots \\
& \quad \sum_{j_m} \sum_{t_1} \cdots \sum_{t_m} h[i_1] \cdots h[i_m] g[l_1] \cdots h[l_m] \\
& \quad \times \overline{h[j_1] \cdots h[j_m] \overline{g[t_1] \cdots h[t_m]}} \\
& \quad \times \left(-\frac{K}{2}\right) [(Q_x + 2^m \tau_x)^2 + (Q_y + 2^m \tau_y)^2]^H \\
& = \Gamma^H \left\{ \sum_{i_1} \cdots \sum_{i_m} \sum_{l_1} \cdots \sum_{l_m} \sum_{j_1} \cdots \right. \\
& \quad \left. \sum_{j_m} \sum_{t_1} \cdots \sum_{t_m} h[i_1] \cdots h[i_m] g[l_1] \cdots h[l_m] \right. \\
& \quad \left. \times \overline{h[j_1] \cdots h[j_m] \overline{g[t_1] \cdots h[t_m]}} \left(-\frac{K}{2}\right) P(\alpha, \beta) \right\} \tag{A6}
\end{aligned}$$

where  $Q_x \equiv i_m + 2i_{m-1} + \cdots + 2^{m-1}i_1 - l_m - 2l_{m-1} - \cdots - 2^{m-1}l_1$  and  $Q_y \equiv j_m + 2j_{m-1} + \cdots + 2^{m-1}j_1 - t_m - 2t_{m-1} - \cdots - 2^{m-1}t_1$ . Let  $\Gamma \equiv (2^m \tau_x)^2 + (2^m \tau_y)^2$ ,  $\alpha \equiv \frac{Q_x}{\Gamma}$ ,  $\beta \equiv \frac{Q_y}{\Gamma}$ ,  $\vec{v} \equiv [Q_x \ Q_y]^T$  and  $P(\alpha, \beta) \equiv [1 + \Gamma \alpha^2 + \Gamma \beta^2 + 2^{m+1} \tau_x \alpha + 2^{m+1} \tau_y \beta]^H$ . Define  $\Omega(\vec{q}) \equiv \{r \mid \sum_{i=1}^2 r_i/q_i \leq 1\}$ ,  $\Omega_0(\vec{q}) \equiv \{r \mid \sum_{i=1}^2 r_i/q_i < 1\}$  and the differentiable closure of  $\Omega_0(\vec{q})$  by  $\bar{\Omega}_0(\vec{q}) \equiv \{r + t \mid r \in \Omega_0(\vec{q}) \text{ and } |t| \leq 1\}$ , where  $\vec{q} \equiv [q_1 \ q_2]^T$ ,  $q_1, q_2 \in \mathbf{R}^+$ . Clearly it is found  $P \in C^{(\infty, \infty)}$  on  $\mathbf{R}^2$ . The Taylor's formula for real-valued  $P(\alpha, \beta)$  at  $(\alpha, \beta) = (0, 0)$  is the following:

$$\begin{aligned}
P(\alpha, \beta) &= \sum_{r \in \Omega} \frac{1}{r!} D^r P(0, 0) (\vec{v})^r \Gamma^{-r} + R_{(0,0)}^{\vec{q}} P(\vec{v} \Gamma^{-1}) \\
&= 1 + 2H(2^m \tau_x Q_x + 2^m \tau_y Q_y) \Gamma^{-1} \\
& \quad + \sum_{r \in \Omega, r_1, r_2 \neq 0, 1} \frac{1}{r!} D^r P(0, 0) (\vec{v})^r \Gamma^{-r} + R_{(0,0)}^{\vec{q}} P(\vec{v} \Gamma^{-1}) \tag{A7}
\end{aligned}$$

where  $R_{(0,0)}^{\vec{q}} P(\vec{v} \Gamma^{-1}) \equiv \sum_{r \in \bar{\Omega}_0 \setminus \Omega} \frac{A_r}{|r|} D^r P(\theta_r \vec{v} \Gamma^{-1}) (\vec{v} \Gamma^{-1})^r$ ,  $D^r$  denotes the partial derivative  $\partial^{|r|} / (\partial \vec{v})^r$ ,  $\{r \in \bar{\Omega}_0 \setminus \Omega\}$  represents  $\{(r \in \bar{\Omega}_0 \cup \Omega) \cap (r \notin \bar{\Omega}_0 \cap \Omega)\}$ , and  $A_r = \sum \{\frac{1}{\gamma!} : \gamma \in \Omega_0 \wedge \gamma + s = r \text{ for some } s \text{ with } |s| = 1\}$ , satisfying  $\theta_r = \theta_\gamma$  whenever

$|r| = |\gamma|$  and  $\lim_{(\alpha, \beta) \rightarrow (0,0)} \frac{R_{(0,0)}^{\vec{q}} P(\alpha, \beta)}{|\alpha|^{q_1} + |\beta|^{q_2}} = 0$  [15, pp. 5–8]. Then we have

$$\begin{aligned}
& [(Q_x + 2^m \tau_x)^2 + (Q_y + 2^m \tau_y)^2]^H \\
& = \Gamma^H P(\alpha, \beta) \\
& = \Gamma^H \left\{ \sum_{r \in \Omega} \frac{1}{r!} D^r P(0, 0) (\vec{v})^r \Gamma^{-r} + R_{(0,0)}^{\vec{q}} P(\vec{v} \Gamma^{-1}) \right\}. \tag{A8}
\end{aligned}$$

Since  $\psi$  has the vanishing moment  $L$ , i.e.,  $\int_{-\infty}^{\infty} t^l \psi(t) dt = 0$ , for  $l = 0, 1, 2, \dots, L-1$ ; or equivalently,  $\sum_k g[k] k^l = 0$ , for  $l = 0, 1, 2, \dots, L-1$  [9, p. 142], therefore, we obtain

$$\begin{aligned}
& R_{D_m^{\text{H}}(B)}[\tau_x, \tau_y] \\
& = (\tau_x^2 + \tau_y^2)^{H-L} \left(-\frac{K}{2}\right) 2^{2m(H-L)} \\
& \quad \times \sum_{i_1} \cdots \sum_{t_m} h[i_1] \cdots h[i_m] g[l_1] \cdots h[l_m] \overline{h[j_1] \cdots h[j_m]} \\
& \quad \times \overline{g[t_1] \cdots h[t_m]} \left\{ \sum_{r \in \Omega, r \geq L} \frac{1}{r!} D^r P(0, 0) (\vec{v})^r 2^{-2m(r-L)} \right. \\
& \quad \left. \times (\tau_x^2 + \tau_y^2)^{-(r-L)} + R_{(0,0)}^{\vec{q}} P(\vec{v} \Gamma^{-1}) \right\}. \tag{A9}
\end{aligned}$$

Because the  $L$ th order partials for  $P(\alpha, \beta)$  depend on  $\tau_x^L$ ,  $\tau_y^L$ , and  $\tau_x^{n_1} \tau_y^{n_2}$ , where  $n_1 + n_2 = L$  and  $n_1, n_2 > 0$ , the  $L$ th order term of  $\{\cdot\}$  in (A6) is bounded below by  $\Gamma^{-\frac{L}{2}}$ . Hence,  $R_{D_m^{\text{H}}(B)}[\tau_x, \tau_y]$  decays as  $\mathcal{O}((\tau_x^2 + \tau_y^2)^{(H-\frac{L}{2}}))$  at least.

Particularly, for the diagonal detail image case, the terms of  $\tau_x^{n_1} \tau_y^{n_2}$ ,  $n_1 + n_2 = L$ , in the autocorrelation function

$$\begin{aligned}
& R_{D_m^{\text{D}}(B)}[\tau_x, \tau_y] \\
& = \Gamma^H \left\{ \left(-\frac{K}{2}\right) \sum_{i_1} \cdots \sum_{t_m} g[i_1] \cdots h[i_m] g[l_1] \cdots \right. \\
& \quad \left. \times h[l_m] \overline{g[j_1] \cdots h[j_m] \overline{g[t_1] \cdots h[t_m]}} P(\alpha, \beta) \right\} \\
& = (\tau_x^2 + \tau_y^2)^{H-L} \left(-\frac{K}{2}\right) 2^{2m(H-L)} \sum_{i_1} \cdots \sum_{t_m} g[i_1] \cdots \\
& \quad h[i_m] g[l_1] \cdots h[l_m] \overline{g[j_1] \cdots h[j_m]} \\
& \quad \times \overline{g[t_1] \cdots h[t_m]} \left\{ \sum_{r \in \Omega, r \geq L} \frac{1}{r!} D^r P(0, 0) (\vec{v})^r 2^{-2m(r-L)} \right. \\
& \quad \left. \times (\tau_x^2 + \tau_y^2)^{-(r-L)} + R_{(0,0)}^{\vec{q}} P(\vec{v} \Gamma^{-1}) \right\} \tag{A10}
\end{aligned}$$

will be vanished by  $g$  after the filter operation along the indices  $i_1, l_1, j_1$  and  $t_1$ . Therefore, the  $L$ th order term of  $\{\cdot\}$  in (A10) is bounded below by  $\Gamma^{-L}$ . Hence,  $R_{D_m^{\text{D}}(B)}[\tau_x, \tau_y]$  decays faster as  $\mathcal{O}((\tau_x^2 + \tau_y^2)^{(H-L)})$ .  $\square$

#### ACKNOWLEDGMENT

The authors thank the anonymous reviewers for providing very helpful comments.

## REFERENCES

- [1] G. Beylkin *et al.*, Eds., *Wavelets and Their Applications*. Cambridge, U.K.: Jones and Bartlett, 1992.
- [2] C. K. Chui, *An Introduction to Wavelets*. New York: Academic, 1992.
- [3] I. Daubechies, "The wavelet transform, time-frequency localization and signal analysis," *IEEE Trans. Inform. Theory*, vol. 36, pp. 961–1005, 1990.
- [4] I. Daubechies, *Ten Lectures on Wavelets*. Philadelphia, PA: SIAM, 1992.
- [5] K. Falconer, *Fractal Geometry: Mathematical Foundations And Applications*. New York: Wiley, 1990.
- [6] P. Flandrin, "Wavelet analysis and synthesis of fractional Brownian motion," *IEEE Trans. Inform. Theory*, vol. 38, pp. 910–917, 1992.
- [7] S. Kandambe and G. F. Boudreaux-Bartels, "A comparison of wavelet functions for pitch detection of speech signals," in *Proc. IEEE Int. Conf. Acoustics, Speech, and Signal Processing*, 1991, pp. 449–452.
- [8] L. M. Kaplan and C.-C. Kuo, "Fractal estimation from noisy data via discrete fractional Gaussian noise (DFGN) and the Haar basis," *IEEE Trans. Signal Processing*, vol. 41, pp. 3554–3562, 1993.
- [9] T. H. Koornwinder, Ed., *Wavelets: An Elementary Treatment of Theory and Applications*. Singapore: World Scientific, 1993.
- [10] H. Krim and J.-C. Pesquet, "Multiresolution analysis of a class of nonstationary processes," *IEEE Trans. Inform. Theory*, vol. 41, pp. 1010–1020, 1995.
- [11] P. Lancaster and M. Tismenetsky, *The Theory of Matrices*, 2nd ed. 1985.
- [12] S. G. Mallat, "A theory for multiresolution signal decomposition: The wavelet representation," *IEEE Trans. Pattern Anal. Machine Intell.*, vol. 11, pp. 674–693, July 1989.
- [13] A. Papoulis, *Probability, Random Variables, and Stochastic Processes*, 3rd ed. New York: McGraw-Hill, 1991.
- [14] H.-O. Peitgen and D. Saupe, Eds., *The Science of Fractal Images*. Berlin, Germany: Springer-Verlag, 1988.
- [15] J.-A. Riestra, *A Generalized Taylor's Formula for Functions of Several Variables and Certain of Its Applications*. Essex, U.K.: Longman House, 1995.
- [16] O. Rioul and M. Vetterli, "Wavelets and signal processing," *IEEE Signal Processing Mag.*, pp. 14–38, Oct. 1991.
- [17] A. Rosenfeld and A. C. Kah, *Digital Picture Processing*, vol. 1, 2nd ed. New York: Academic, 1982.
- [18] A. H. Tewfik and M. Kim, "Correlation structure of the discrete wavelet coefficients of fractional Brownian motion," *IEEE Trans. Inform. Theory*, vol. 38, pp. 904–909, 1992.
- [19] A. M. Yaglom, *Correlation Theory of Stationary and Related Random Functions I: Basic Results*. Berlin, Germany: Springer-Verlag, 1986.